

PARTICLE-SIZE DISTRIBUTION INFLUENCE IN HIGH-SPEED EROSION OF ALUMINIUM

ANDREAS W. MOMBER
WOMA Apparatebau GmbH
P.O. Box 141820
D-47208 Duisburg
Germany

RADOVAN KOVACEVIC
Department of Mechanical Engineering
Southern Methodist University
P.O. Box 750337
Dallas, TX 75275-0337, USA

ABSTRACT

The paper discusses the influence of the abrasive particle-size distribution on typical high-speed abrasive-waterjet erosion parameters. The size distributions of the used abrasive particles are modelled by a Rosin-Rammler-Sperling (RRSB) grain-size distribution containing the distribution parameters D and n . Both parameters are independently varied to characterise different particle-size distributions. Aluminium specimens are eroded by abrasive-waterjets at velocities of 320 m/s, and the erosion depth, depth distribution, and the surface roughness are measured. The depth distribution and the surface roughness are very sensitive to the particle-size distribution parameters, whereas the average erosion depth is not influenced significantly. These results offer the possibility to select an „optimum“ grain-size distribution for maximum surface quality at fixed kinematics conditions.

1. INTRODUCTION

As a new manufacturing process, high-speed abrasive-waterjet erosion has been very effective in machining difficult-to-machine materials. This technique is one of the most recently introduced machining methods. It is used for machining a wide range of materials, including ceramics and composite materials; it also has potentials in milling operations and 3-D-machining. Typical applications are described by Kovacevic and Yong (1996), Momber and Kovacevic (1998) and Momber et al. (1996). A commercial system consists of a pressure generator, typically an intensifier pump, an abrasive machining head, a x-y-z-positioning system, and a catcher.

Depending on the jet generation, abrasive waterjets can generally be categorized as injection jets or suspension jets (Momber and Kovacevic, 1998). For practical applications, injection jets are more commonly used. For this type of jet, the pressure ranges from $p=200$ MPa up to $p=400$ MPa. The jet is formed by accelerating small abrasive particles (garnet, aluminum oxide, silica carbide) through contact with a high-velocity waterjet. A typical abrasive-particle diameter is $d_p=400$ μm . Whereas, the waterjet is formed in an orifice on top of the head, the abrasives enter the head at a separate entry. The mixing between abrasives, waterjet, and air takes place in a mixing chamber, and the acceleration process occurs in an acceleration tube. The particles leave this nozzle at velocities of several hundred meters per second. A high number of particles (10^5 per second) leads to a high-frequency impingement on the materials being eroded. This process is discussed in detail by Momber and Kovacevic (1998).

Based on detailed observations in transparent materials, Hashish (1988a) first discussed the material-removal mechanisms in abrasive-waterjet erosion, and subdivided the process into two stages. In the first stage, the particles strike the surface at a shallow angle producing a relatively smooth surface. The secondary region, displaying unsteady erosion with striation marks, is controlled by erosive wear due to particles impacting at large angles of attack. The early characterization of these zones as „cutting-wear zone" and „deformation-wear zone" as suggested by Hashish (1988a) is discussed controversially because it suggests two different mechanisms of material removal in a single kerf. Therefore, in the actual literature the terms „smooth-cutting zone", characterized by roughness, and „rough-cutting zone", characterized by waviness and striations, are used to distinguish between both stages (see Fig. 2a). As stated by Raju and Ramulu (1994), the transition point between the two stages is dictated by the local kinetic energy of the particle-water slurry. The aim of the present paper is to investigate the effect of the particle-size distributions on the quality of the „smooth cutting zone".

Efficiency and quality of the erosion process depend on several process parameters, such as particle velocity, orifice diameter, traverse rate, local erosion time, standoff distance, mixing-chamber geometry, abrasive mass-flow rate, and abrasive type. Whereas, the impact of these parameters on the erosion is extensively discussed in the reference literature (Hashish, 1988b, Momber and Kovacevic, 1998), almost no attention is given to the particle-size distribution parameters of the abrasive materials.

Commercially used abrasive materials are comminution products. To determine the particle-size distribution of comminution products, a number of equations has been developed. A review is given by Kelly and Spottiswood (1982). These equations are all of the generalized type,

$$M(d_p) = f \left[\frac{d_p}{D} \right]^n \quad (1)$$

Here, M is the cumulative sieve-overflow mass, and d_p is the corresponding particle diameter. The higher M for a given sieve diameter the more particles have a diameter smaller than d_p . The parameter D is frequently referred to as the size modulus. The exponent n is called the distribution modulus since it is a measure of the spread of the individual particle sizes in the grain sample.

In the state-of-the-art erosion optimization, the size modulus D was investigated by several researchers in terms of an average particle diameter as will be pointed out in the next Section.

Although the distribution modulus n contains information about the regularity of the applied particle collection and about the loading regime, it is completely neglected in previous studies. It is the objective of this paper to show how both the particle-size distribution parameters - the size modulus, and the distribution modulus - can influence efficiency and quality of an abrasive waterjet erosion process.

2. PARTICLE-SIZE INFLUENCE ON THE EROSION PROCESS - A REVIEW

To evaluate the influence of the abrasive particle-size distribution, it is useful to distinguish between the mixing-and-acceleration process in the abrasive machining head, and the material-removal process in the workpiece.

It can be assumed that any mixing process is related to a corresponding optimum particle-size distribution. Under this optimum condition, the particles are accelerated up to a maximum velocity, and the fragmentation of the individual grains is minimized. It was found by Heßling (1988) that heavy (large) particles require a larger acceleration distance (increased focus length) compared to smaller particles. Mazurkiewicz et al. (1988) concluded from piercing experiments a relationship between the particle size and the optimum diameter of the focusing nozzle. A general problem in evaluating the influence of the grain size is the fragmentation of the original particles during the acceleration process as observed and discussed among others by Simpson (1990). Therefore, the particle-size distribution at the impact zone is not identical with the original particle-size distribution.

Neglecting these relations and assuming identical particle velocities, it can generally be stated that larger particles are characterized by higher kinetic energy due to their higher mass. This generates deeper kerfs up to a certain particle diameter. On the other hand, an increase in the particle size leads to a decrease in the particle number for a given abrasive mass-flow rate. This results in a lower impinging frequency. For materials that are very sensitive to the impact frequency (such as materials that absorb a certain amount of energy before they fail), these relationships suggest an optimum average particle diameter which was in fact observed for aluminum (Faber and Oweinah, 1991) and copper (Hashish, 1984), but also for quasi-brittle, pre-cracked materials, such as rocks (Heßling, 1988).

Systematic investigations into the particle-size influence on the roughness of the generated erosion walls were carried out by Kovacevic (1989) and Webb and Rajukar (1990). Based on SEM-observations, both references found wear tracks plowed into the „smooth-cutting zone“ by individual particles. The width of these tracks is non-uniform and is related to the particle diameter. Kovacevic (1989) observed that the wear tracks follow vertical lines in the upper region of the wall. Webb and Rajukar (1990) as well as Kovacevic (1989) developed regression models for the calculation of the roughness. Kovacevic (1989) suggested a direct relationship between the roughness and the Mesh-number of the particles, whereas Webb and Rajukar (1990) found a relationship $Ra \sim d_p^{0.45}$. Direct measurements of the roughness for a particle-size range between $d_p=50 \mu\text{m}$ and $d_p=600 \mu\text{m}$ performed by Zhou et al. (1992) and Gou et al. (1993, 1994) verified these trends.

Zhou et al. (1992) discussed the surface structure of the „smooth-cutting zone“ as a superposition of micro-dimples created by individual particles, which is in general the same philosophy as discussed above. Using auto-correlation functions, surface-height distributions, and isotropic criteria, they concluded that the surface topography of this zone is random, Gaussian, and weakly isotropic. Kovacevic et al. (1993) used the time-series modeling

technique and detected two different types of wave length which are responsible for the surface profile of abrasive-waterjet eroded surfaces. The secondary wavelength is linked to the abrasive particles. A very similar result was obtained in a study by Guo et al. (1994) where a Fourier-transformation technique was used. Ramulu and Arola (1994) who investigated the surface quality of composite materials eroded by abrasive-waterjets found that the grain size has the predominant influence on the surface roughness. They also observed a decrease in the roughness with decreasing particle size.

In a fundamental study about the surface roughness, Singh et al. (1994) found that the influence of the particle size (given in mesh designation) on the roughness depends on the erosion depth. For a shallow erosion depth, typically in the range of the "smooth-cutting zone", roughness increases as particle size increases. However, for a deeper erosion the relationships are more complex.

3. PARTICLE-SIZE DISTRIBUTION PARAMETERS OF THE USED ABRASIVE MIXTURES

The abrasive material used for the study was a commercial product with the trade name „Barton Garnet“. Chemical composition as well as physical properties of the material are listed in Table 1. Figure 1a provides a close view on a sample.

The particle-size distributions of the abrasive mixtures used in this study were designed by applying a Rosin-Rammler-Sperling (RRSB)-distribution, which is commonly used to characterize fine-grained particle mixtures (Kelly and Spottiswood, 1982). This type of distribution is given by,

$$M = 100 \cdot \exp \left[- \left(\frac{d_p}{D} \right)^n \right] \quad (2)$$

It is characterized by the distribution parameters D and n . The size modulus D is a characteristic grain diameter for $M=36.8\%$ and, under some limitations, describes the fineness of the grain samples. In this paper, D is used as an average grain diameter of the abrasive material. The distribution modulus n is a regularity number; for conventional comminution products, this parameter ranges between $n=0.7$ and $n=1.4$ (Kelly and Spottiswood, 1982). In the range $n>1$, it describes the homogeneity of the particle-size distribution. The value for n is infinite if the sample consists of particles with identical diameters. For grain samples with a wide range of different grain diameters, n is small. Eq. (2) can be rewritten,

$$\frac{100}{M} = \exp \left[\left(\frac{d_p}{D} \right)^n \right] \quad (3)$$

After logarithmizing Eq. (3) twice, one obtains a linear relationship,

$$\lg \left[\lg \left(\frac{100}{M} \right) \right] = \underbrace{n}_{A} \cdot \underbrace{\lg d_p}_{X} + \underbrace{\frac{C_1}{B}}_{B} \quad (4)$$

In this equation, $A=n$, and $B=\lg(\lg e)-n \cdot \lg D$. If the results of a sieve analysis fits Eq. (4), it can be characterized by an RRSB-distribution. Eqs. (1) to (4) were used in this paper for the design of the particle-size distributions. For the design, four different levels of the size modulus D (for one constant level of the distribution modulus), and five different levels of the distribution modulus n (for one constant level of the size modulus) were fixed as listed in Table 2. Therefore, nine different particle mixtures were designed for this study.

After fixing the distribution parameters, the grain samples were designed using Eq. (2). For every given set of D - n , the individual mass fractions $M(d_p)$ were calculated for the sieve-size series ($d_p =$ 53, 106, 150, 250, 420, and 500 μm). These mixtures were used for the erosion experiments. Some examples of the designed distributions are shown in Fig. 1b.

4. EXPERIMENTAL SETUP AND PROCEDURE

The abrasive-waterjet erosion unit used in this study consisted of an intensifier pump, an abrasive machining head, an abrasive storage and metering system, a catcher, and a x-y-z-positioning table. The erosion conditions are listed in Table 3. As specimens, aluminum Al 2024 samples were used with the dimensions $L=80$ mm and $B=25$ mm.

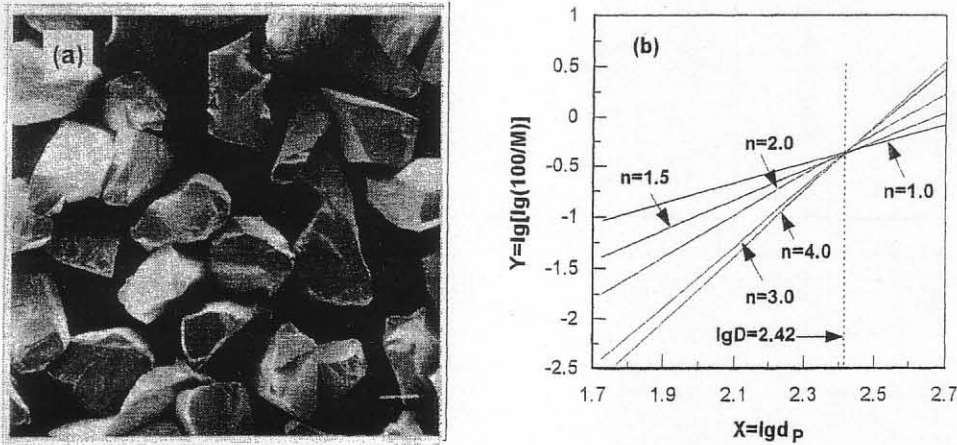


Figure 1 Properties of abrasive mixtures used in the study: (a) SEM-image of the mixture 3 (scale: 200 μm), and (b) RRSB-distribution plots of selected mixtures

Table 1. Technical Data and Physical Characteristics for the Used Abrasive Material (Barton Mines Corp., North Creek)

Feature	Comments
General Description	<ul style="list-style-type: none"> - Combination of almandite and pyrope - Homogeneous mineral - No free chemicals - Oxides and dioxides are combine chemically as follows: $\text{Fe}_3\text{Al}_2(\text{SiO}_4)_3$ - Iron and aluminum ions are partially replaceable by calcium, magnesium, and manganese
Chemical Analysis	<ul style="list-style-type: none"> - Silicon Dioxide (SiO_2) 41.34 % - Ferrous Oxide (FeO) 9.72 % - Ferric Oxide (Fe_2O_3) 12.55 % - Aluminum Oxide (Al_2O_3) 20.36 % - Calcium Oxide (CaO) 2.97 % - Magnesium Oxide (MgO) 12.35 % - Manganese Oxid (MnO) 0.85 %
Hardness	Between 8 and 9 on Mohs scale
Strength	Friable to tough
Particle shape	Sharp, angular, irregular
Cleavage	Pronounced laminations, irregular cleavage planes
Color	Red to pink
Streaks	White
Transparency	Translucent
Lustre	Vitreous
Specific gravity	3.9 g/cm ³ to 4.1 g/cm ³
Mean refractive index	1.83
Facet angles	37 °C and 42 °P
Crystallization	Cubic (isometric) system as rhombic dodecahedrons or tetragonal trisectahedrons (trapezohedrons) or in combinations of the two
Melting Point	1,315 °C (2,300 °F)
Magnetism	Slightly magnetic (volume susceptibility = 9.000375)
Electrostatic properties	<ul style="list-style-type: none"> - Mineral conductivity: 18,000 volts - Non-reversible
Moisture absorption	Non-hygroscopic, inert
Dispersion	Self-dispersing
Uniformity	Garnet mineral in the deposit was formed simultaneously under identical natural conditions. It has been proven uniform throughout during over 100 years of use in technical abrasive applications.
Harmful free silica content	None (silicosis free)

Table 2. Particle-Size Distribution Parameters

Mixture	1	2	3	4	5	6	7	8	9
D [μm]	250	250	250	250	250	400	250	200	150
n	1.0	1.5	2.0	3.0	4.0	1.5	1.5	1.5	1.5

The abrasive metering system was calibrated for every particle mixture to obtain an identical abrasive mass-flow rate ($m_A=8.3$ g/s). Two sets of experiments were carried out. First, the aluminum samples were eroded using the different particle mixtures. Then, the average erosion depth as well as the depth distribution were estimated. The average erosion depth was calculated from 20 measurements along the erosion track. Here, the entry zone and the exit zone of the kerfs were excluded. In the second part of the experiment, the quality of the generated surfaces was analyzed by measuring the roughness. A mechanical roughness measurement unit was used with different cut-offs. The profile length was 12.5 mm for all samples.

Table 3. Conditions for the Erosion Experiments

Parameter	Unit	Value
Pump pressure	MPa	250
Particle velocity	m/s	ca. 320
Traverse rate	mm/s	0.8
Local erosion time	s	0.3
Abrasive mass-flow rate	g/s	8.3
Orifice diameter	mm	0.23
Focus diameter	mm	1.6
Abrasive type	Garnet	-

5. EXPERIMENTAL RESULTS AND DISCUSSION

5.1 Influence on Depth of Cut

The erosion depth over the sample length was generally unsteady and random. Based on the 20 measurements along the erosion line, the depth distribution was estimated by plotting the frequency of the depth against a certain class of depth. The class width was 5.0 mm, the number of classes was 7.

As Fig. 2b shows, the erosion-depth distribution can be characterized by a Gaussian Normal Distribution (GND),

$$f(h) = \frac{1}{\sqrt{2 \cdot \pi \cdot \sigma_h}} \cdot \exp \left[-\frac{(h - \bar{h})^2}{2 \cdot \sigma_h^2} \right] \quad (5)$$

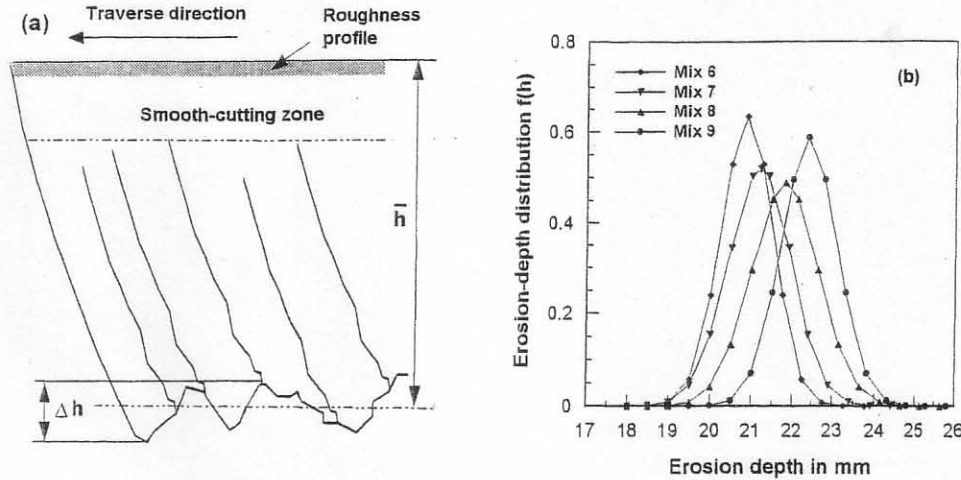


Figure 2 Erosion process and target parameter definition (a), and erosion-depth distributions for different particle-size distribution parameters (b)

In Eq. (5), \bar{h} is the average erosion depth (see Fig. 2a). The parameter σ_h is the standard deviation of the erosion depth,

$$\sigma_h = \sqrt{\frac{1}{N-1} \sum_{i=1}^N (h_i - \bar{h})^2} \quad (6)$$

Figure 3 shows the relationship between the average erosion depth, measured in the material, and the grain-size distribution parameters. A reduced size modulus D leads to deeper kerfs for constant values of n (Fig. 3a). This could be due to the higher number of impacting particles on the aluminum surface. Assuming spherical abrasive particles, the number of impacting particles, N_p , is,

$$N_p = \frac{6 \cdot m_A \cdot t_E}{\pi \cdot D^3 \cdot \rho_A} \quad (7)$$

Thus, $N_p \sim 1/D^3$. Here, ρ_A is the abrasive material density, m_A is the abrasive mass-flow rate, and t_E is the erosion time. Aluminum as a material showing ductile behavior is removed by accumulated micro-cutting or micro-ploughing performances due to single particle impacts. A higher number of impacting particles, therefore, removes more material as far as the kinetic energy of the particle exceeds a critical threshold energy. The opposite trend was observed for the distribution parameter n for constant values of D (Fig. 3b). The erosion depth increases slightly with an increase in the regularity of the particle mixture. This is probably due to the fact that the mixtures with high values of n contain less fine-grained particles which are usually inefficient in the material removal process.

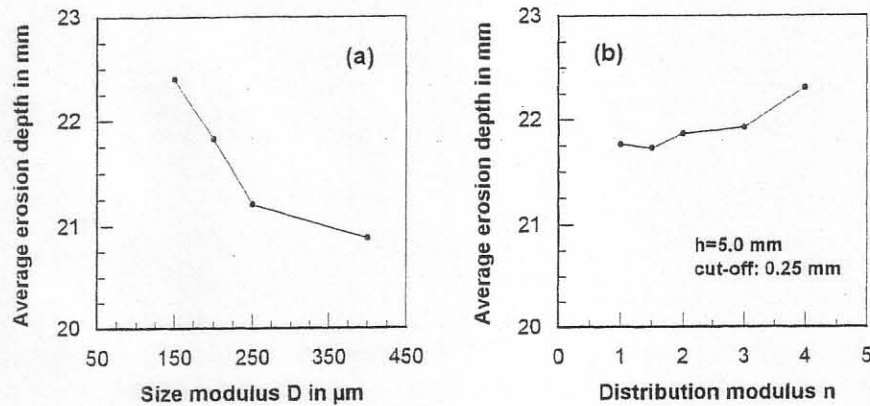


Figure 3 Particle-size distribution parameter influence on the average erosion depth

The difference between the shallowest kerf and the deepest kerf is about 8 % for the size modulus as variable parameter (Fig. 3a), and about 2 % for the distribution modulus as variable parameter (Fig. 3b). Both values are not significant. Thus, the particle-size distribution parameters do not influence the erosion depth from the practical point of view. However, there exists an abrasive mixture for a maximum erosion capability with the distribution parameters $D=150 \mu\text{m}$ and $n=1.5$ (mixture 9). The influence of the size modulus D on the erosion depth is more intense.

The particle-size parameters affect also the standard deviation of the erosion depth. This is shown in Fig. 4. The maximum difference in the standard deviation is 30 % for D as the variable parameter (Fig. 4b). For the distribution modulus n , the maximum difference in the standard deviations is about 70 % which is significant. Thus, the regularity of the depth profile is more affected by the distribution modulus. There is no general trend, but it seems that a mixture with a smaller distribution modulus generates a more regular depth structure (Fig. 4a). This result was not necessarily expected. One would expect a more regular depth distribution with a higher particle-mixture regularity. Possibly, the particle fragmentation process inside the focusing nozzle plays a role here. The fragmentation process may vary the structure of the particle sample in a way that the fineness tendency remains (that means the trend of the size modulus of the mixtures is the same before mixing and after mixing) but the regularity of the particle mixture changes. This is a very interesting point for further research. It could also be assumed that the influence of the particle size is canceled due to the influence of the waterjet geometry in the bottom region of the kerf (Kovacevic et al., 1993). The influence of the size modulus D on the standard deviation is shown in Fig. 4b. For the largest value of the size modulus, the smallest standard deviation is achieved. But the standard deviation is also low for the smallest value of D . The most regular depth profile is generated by the parameter combination $D=400 \mu\text{m}$, and $n=1.5$. The results of this part of the investigation are very important for the milling operations in terms of quality optimization of the bottom surface of a milled pocket.

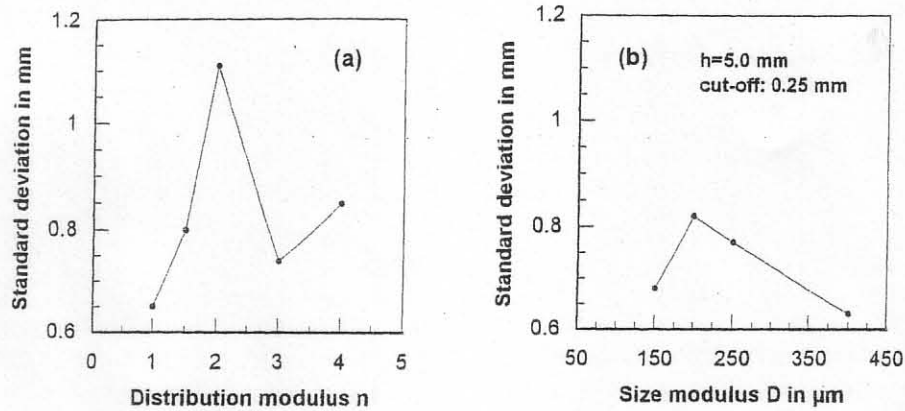


Figure 4 Particle-size distribution parameter influence on the erosion depth profile

5.2 Influence of Surface Roughness

Figure 5 exhibits the relationship between the particle-size distribution parameters and the roughness of the kerf walls measured at a distance of $h=5.0$ mm from the top of the cut (see Fig. 2a). Characteristic plots from the roughness measurements are shown in Figs. 6 and 7. As expected, the roughness depends on both distribution parameters. The average roughness tends to increase with an increase in the size modulus (Fig. 5b) which is in agreement with results of previous investigations (see Section 2), and supports the hypothesis that the fragmentation process in the focusing nozzle will not alter the general trend of the size modulus. This result is in particular in good qualitative agreement with the relationship $R_a \sim d_p^{0.45}$ as derived by Webb and Rajukar (1990).

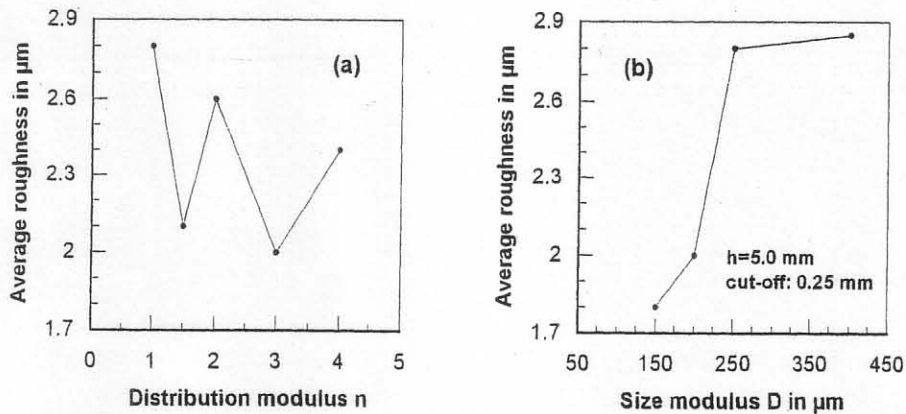


Figure 5 Particle-size distribution parameter influence on the average surface roughness

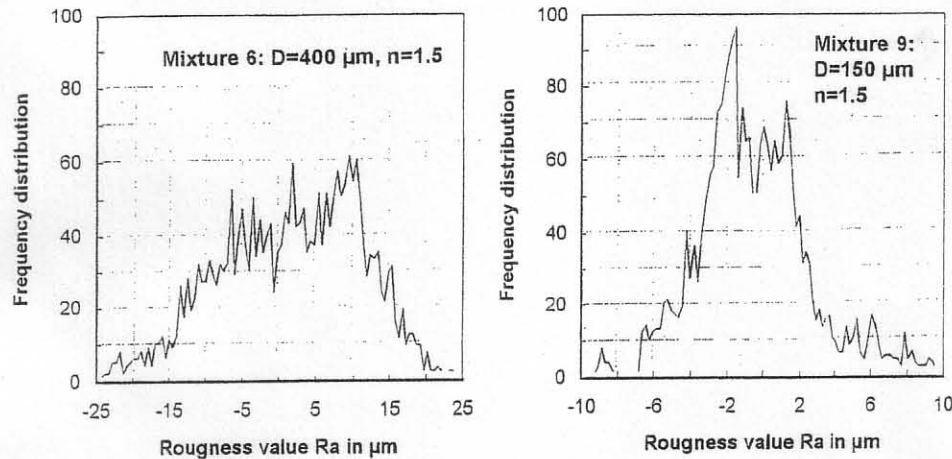


Figure 6 Amplitude distributions for different particle distribution parameters ($h=10$ mm)

The influence of the distribution modulus on the average roughness does not show any clear trend (Fig. 5a). However, it is less significant than that of the size modulus. The maximum difference in the average roughness values is about 40 % for the distribution modulus, and about 60 % for the size modulus. The optimum parameter combination for achieving the minimum roughness is $D=150$ μm , and $n=1.5$ (mixture 9).

Figure 6 shows some amplitude distributions measured at an erosion depth of $h=10$ mm and with a cut-off of 2.5. The amplitude distribution is comparatively wide for mixtures with a low distribution modulus and a high size modulus. The gradation of the amplitude distribution curve increases with an increase in the distribution modulus and a decrease in the size modulus. The most regular roughness profile can be generated by the parameter combination $D=250$ μm , and $n=4$ (mixture 5).

6. SUMMARY AND CONCLUSIONS

Through the performed study it is shown the following:

- The influence of two particle-size distribution parameters, a size modulus ($D=150$ μm to $D=400$ μm) and a distribution modulus ($n=1.0$ to $n=4.0$), on the erosion of aluminum by abrasive-waterjets is investigated for the first time. The distribution parameters are derived from a Rosin-Rammler-Sperling (RRSB) grain-size distribution.
- The influence of these parameters on the erosion depth is not significant in the given parameter range. The maximum difference in the erosion depth is about 8 %.
- The distribution of the erosion depth follows a Gaussian Normal-Distribution. The influence of the particle-size distribution parameters on the standard deviation is significant. The standard deviation changes up to 70 % using different distribution moduli.

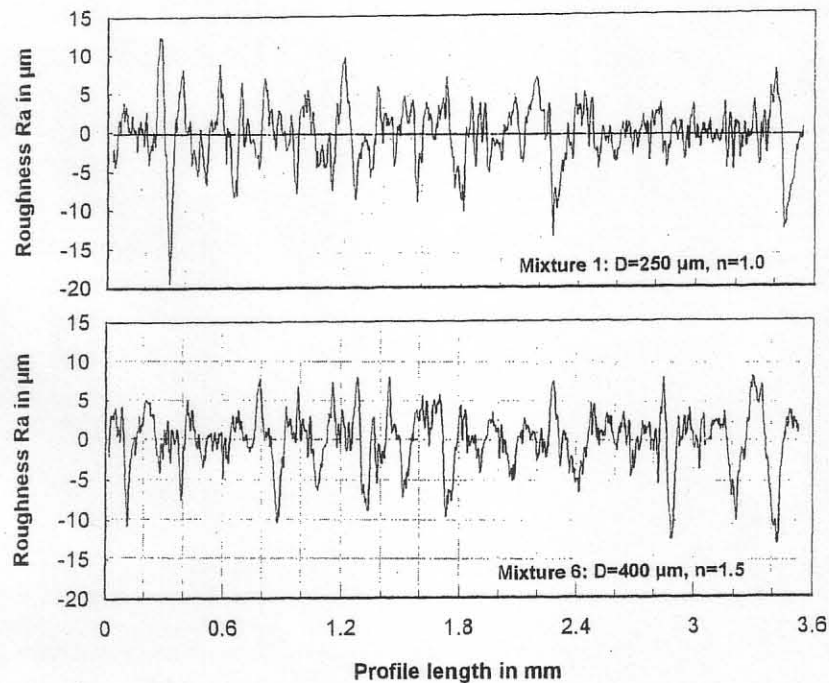


Figure 7 Typical roughness profile plots ($h=10$ mm, cut-off: 0.25 mm)

- The roughness of the eroded surface in the „smooth-cutting zone“ is sensitive to changes in both of the particle-size distribution parameters. The maximum difference in the measured roughness is about 60 % for different distribution moduli, and about 40 % for different size moduli.
- An „optimum“ particle-size distribution exists for the abrasive-waterjet erosion of aluminum in the given parameter range. In this study, this optimum is characterized by the distribution parameters $D=150$ μm and $n=1.5$.
- For a given erosion depth, the quality of the erosion process (depth variation, surface roughness) can be significantly improved by selecting the optimum particle-size distribution parameters.
- The preliminary results of this paper have shown that the quality of an abrasive waterjet erosion process can be improved significantly without any further increase in the system energy. Additional studies may be required to statistically prove the trends observed and discussed in this study.

ACKNOWLEDGEMENTS

The authors are thankful to the Alexander von Humboldt-Foundation, Bonn, Germany, and to the German Research Association, Bonn, Germany, for financial support.

REFERENCES

- Faber, K., and Oweinah, H., 1991, Influence of process parameters on blasting performance with the abrasive jet, in D. Saunders, (ed.), *Jet Cutting Techn.*, Elsevier, London, pp. 365-382.
- Guo, N.S., Louis, H., and Meier, G., 1993, Surface structure and kerf geometry in abrasive water jet cutting: formation and optimization, in M. Hashish, (ed.), *Proc. 7th Amer. Water Jet Conf.*, Vol. 1, Water Jet Techn. Ass., St. Louis, pp. 1-25.
- Guo, N.S., Louis, H., Meier, G. and Ohlsen, J., 1994, Modeling of abrasive particle disintegration in abrasive water jet cutting in relation to the recycling capacity, in N.G. Allen, (ed.), *Jet Cutting Techn.*, Mech. Eng. Publ., London, pp. 567-587.
- Hashish, M., 1984, A modeling study of metal cutting with abrasive water jets, *Trans. ASME, J. Eng. Mat. and Techn.*, Vol. 106, pp. 88-100.
- Hashish, M., 1988a, Visualization of the abrasive waterjet cutting process, *Exper. Mechan.*, Vol. 28, 159-169.
- Hashish, M., 1988b, Optimization factors in abrasive-waterjet machining, *ASME-PED*, Vol. 34, pp. 163-180.
- Heßling, M., 1988, Basic investigations into the cutting of rocks by abrasive water jets (in German), Ph.D. dissertation, RWTH Aachen, Aachen, Germany.
- Kelly, E.G. and Spottiswood, D.J., 1982, *Introduction to Mineral Processing*, Wiley, New York.
- Kovacevic, R. and Yong, Z., 1996, Modelling of 3D abrasive waterjet machining, in C. Gee, (ed.) *Jetting Techn.*, Mechan. Engng. Publ. Ltd., London, pp. 83-90.
- Kovacevic, R., 1989, Surface texture in abrasive water jet cutting, *J. of Manufact. Syst.*, Vol. 10, pp. 32-40.
- Kovacevic, R., Mohan, R., and Zhang, Y., 1993, Stochastic modeling of surface texture generated by high energy jets, *Proc. Inst. Mech. Engrs., J. of Engng. Manuf.*, Vol. 207, pp. 129-140.
- Mazurkiewicz, M., Fincuan, L. and Ferguson, R., 1988, Investigation of abrasive cutting head internal parameters, in P.A. Woods, (ed.), *Proc. 9th Int. Symp. Jet Cutting Techn.*, BHRA, Cranfield, pp. 75-84.
- Momber, A.W. and Kovacevic, R., 1998, *Principles of Abrasive Water Jet Machining*, 1st ed., Springer Ltd., London.
- Momber, A.W., Eusch, I. and Kovacevic, R., 1996, Machining refractory ceramics with abrasive water jets, *J. Materials Sci.*, Vol. 31, pp. 6485-6493.
- Raju, S.P. and Ramulu, M., 1994, Predicting hydro-abrasive erosive wear during abrasive waterjet cutting: part II - an experimental study and model verification, *ASME-PED*, Vol. 68-1, pp. 381-396.
- Ramulu, M., and Arola, D., 1994, The influence of abrasive waterjet cutting conditions on the surface quality of graphite/epoxy laminates. *Int. J. Tools Manuf.*, Vol. 34, pp. 295-313.
- Simpson, M., 1990, Abrasive particle study in high pressure water jet cutting, *Int. J. Water Jet Techn.*, Vol. 1, pp. 17-28.
- Singh, P.J., Chen, W.L. and Munoz, J., 1994, Comprehensive evaluation of abrasive water jet cut surface quality. *Int. J. of Water Jet Techn.*, Vol. 2, pp. 11-27.

- Webb, K.E. and Rajurkar, K.P., 1990, Surface characterization of inconel cut by abrasive water jet, in Proc. CSME Mech. Engng. Forum, 1990.
- Zhou, G., Geskin, E.S. and Chung, Y.C., 1992, Investigation of topography of waterjet generated surfaces, ASME-PED, Vol. 62, pp. 191-202.